

Improved Finite-Difference Schemes for Transonic Potential Flow Calculations

M. Hafez*

University of California at Davis, Davis, California

W. Whitlow Jr.†

NASA Langley Research Center, Hampton, Virginia

and

S. Osher‡

University of California at Los Angeles, Los Angeles, California

A modified artificial density method based on flux biasing is used to solve the full potential equation in conservation form. It is shown that expansion shocks are not allowed with the present scheme. Typical numerical results are presented.

Introduction

IN 1980, Engquist and Osher¹ introduced a finite-difference scheme for solving the transonic small-disturbance equation, such that only compression shocks are admitted. Some attempts to generalize the Engquist-Osher (E-O) scheme for the full potential equation are reported in Refs. 2-5. In Ref. 6, the authors study a class of such schemes and prove rigorously that rules out expansion shocks. The new "entropy" function for the full potential formulation is related to a pseudo-unsteady symmetric hyperbolic system and, using the results of Lax⁷ and Friedrichs and Lax,⁸ the required inequality is established. The analysis of Ref. 6 is restricted, however, to steady two-dimensional flows.

In the present work, a heuristic approach is adopted. It is known that expansion shocks are associated with negative drag that, for potential flow, can be expressed in terms of momentum losses. The artificial dissipation in the present scheme leads, however, to a positive drag. Hence, expansion shocks are not possible. The argument is not restricted to symmetric hyperbolic systems nor to steady two-dimensional flows.

One-Dimensional Flows

As a starting point, a one-dimensional problem is considered. For example,

$$\frac{1}{2} (u^2)_x = (\epsilon u_x)_x \quad (1)$$

admits expansion as well as compression shocks when $\epsilon = 0$. When $\epsilon > 0$, expansion shocks are not possible. This can be seen in the following discussion. Multiplying Eq. (1) by u and integrating by parts yields

$$\frac{1}{3} [u^3] = [u \epsilon u_x] - \int_{x_1}^{x_2} \epsilon u_x^2 dx \quad (2)$$

where $[(\)] = (\)_2 - (\)_1$.

Presented as Paper 84-0092 at the AIAA 22nd Aerospace Sciences Meeting, Reno, NV, Jan. 9-12, 1984; received Feb. 28, 1986; revision received Feb. 18, 1987. Copyright © American Institute of Aeronautics and Astronautics, Inc., 1987. All rights reserved.

*Professor, Department of Mechanical Engineering, Associate Fellow AIAA.

†Aerospace Engineer, Unsteady Aerodynamics Branch, Member AIAA.

‡Professor of Mathematics, Member AIAA.

Assuming that the first term on the right-hand side of Eq. (2) is negligible, it is clear that u has to decrease across a shock since

$$\begin{aligned} [u^3] &= \langle u^2 \rangle [u] + \langle u \rangle [u^2] \\ &= (\langle u^2 \rangle + 2\langle u \rangle^2) [u] \end{aligned} \quad (3)$$

where $\langle (\) \rangle = \frac{1}{2} [(\)_2 + (\)_1]$.

The quantity $-[u^3]$ is related to the drag.⁹⁻¹² In the above example, the discontinuity is replaced by a smooth transition (where the gradient in the regions is large).

The shock in the numerical solution of Eq. (1) is usually smeared over many points. To obtain a sharp shock, the viscosity coefficient may be switched off in the subsonic region, as for example in the Murman¹³ and the Engquist-Osher (E-O) schemes. Following Jameson,¹⁴ Murman's scheme is represented by

$$(u^2)_x = (\nu (u^2)_x)_x \Delta x \quad (4)$$

where ν is a discontinuous function

$$\begin{aligned} \nu &= 0 & u \leq 0 \\ &= 1 & u > 0 \end{aligned}$$

The shock point operator of Murman is completely equivalent to fitting a locally normal shock as shown in Ref. 15. Indeed, the distinction between such new schemes and classical shock-fitting methods becomes less clear as discussed by Moretti in Ref. 16. However, the actual discrete form of Eq. (4) admits an expansion shock at $u = 0$. In this case, the associated entropy and drag are negative. On the other hand, the E-O scheme is defined by Eq. (5) where

$$\frac{1}{2} (u^2)_x = \frac{1}{2} (v_x^2)_x \Delta x \quad (5)$$

and

$$\begin{aligned} v &= u & u > 0 \\ &= 0 & u \leq 0 \end{aligned}$$

Here, the associated drag is always positive. In the case of the full potential equation, the E-O scheme is related to

$$f_x = F_{xx} \Delta x \quad (6)$$

where

$$\begin{aligned} f &= \rho u \\ F &= f \quad M > 1 \\ &= f^* = \rho^* u^* \quad M \leq 1 \end{aligned}$$

In the above, ρ is the density, M is the local Mach number, and $()^*$ denotes the sonic condition. It is shown in Ref. 1 that only compression shocks are admitted, with a maximum of two points in the shock region.

Numerical Examples

The E-O scheme is easy to implement and has a continuously differentiable flux function. First, the following Newton's linearization is considered

$$(\delta \rho u)_x = -(\rho u)_x \quad (7)$$

where

$$\begin{aligned} u &= \phi_x \\ \delta u &= \delta(\phi_x) = (\delta \phi)_x \\ \delta \rho u &= \rho [1 - (u^2/a^2)] \delta u \end{aligned}$$

The quantities δu and $\delta \phi$ are the corrections to u and ϕ , respectively. Hence, Eq. (7) reads

$$\left[\rho \left(1 - \frac{u^2}{a^2} \right) (\delta \phi)_x \right]_x = -(\rho \phi_x)_x \quad (8)$$

If central differences are used, Eq. (8) becomes

$$\begin{aligned} c_{i+1/2}(\delta \phi_{i+1} - \delta \phi_i) - c_{i-1/2}(\delta \phi_i - \delta \phi_{i-1}) \\ = -\rho_{i+1/2}(\phi_{i+1} - \phi_i) + \rho_{i-1/2}(\phi_i - \phi_{i-1}) \end{aligned} \quad (9)$$

where

$$c_{i+1/2} = \rho_{i+1/2} \left(1 - \frac{u_{i+1/2}^2}{a_{i+1/2}^2} \right)$$

For supersonic flows, the artificial viscosity leads to an upwind difference scheme of the form

$$\begin{aligned} c_{i-1/2}(\delta \phi_i - \delta \phi_{i-1}) - c_{i-3/2}(\delta \phi_{i-1} - \delta \phi_{i-2}) \\ = -\rho_{i-1/2}(\phi_i - \phi_{i-1}) + \rho_{i-3/2}(\phi_{i-1} - \phi_{i-2}) \end{aligned} \quad (10)$$

In general, in E-O discretization, there are two parabolic point operators and two shock point operators.

At the first parabolic point (just upstream of the sonic point), the discrete equation for the correction is

$$-c_{i-1/2}(\delta \phi_i - \delta \phi_{i-1}) = -\rho^* u^* \Delta x + \rho_{i-1/2}(\phi_i - \phi_{i-1}) \quad (11)$$

The corresponding equation for the second parabolic point (just downstream of the sonic point) is

$$c_{i-1/2}(\delta \phi_i - \delta \phi_{i-1}) = -\rho_{i-1/2}(\phi_i - \phi_{i-1}) + \rho^* u^* \Delta x \quad (12)$$

Note the difference in signs in Eqs. (11) and (12). In both equations, the left-hand side can be interpreted as an approximation of a ϕ_{xx} term, while the right-hand side is an approximation of $-\rho \phi_x = -\rho(1-M^2)\phi_{xx}$. The proper sign of the coefficient of the ϕ_{xx} term is automatically chosen at the

sonic points. It can be shown that Eq. (11) is consistent with Eq. (9) and Eq. (12) with Eq. (10).

On the other hand, at the first shock point, the equation for the correction is

$$\begin{aligned} c_{i-1/2}(\delta \phi_i - \delta \phi_{i-1}) - c_{i-3/2}(\delta \phi_{i-1} - \delta \phi_{i-2}) + c_{i+1/2}(\delta \phi_{i+1} - \delta \phi_i) \\ = -(\rho_{i-1/2}(\phi_i - \phi_{i-1}) - \rho_{i-3/2}(\phi_{i-1} - \phi_{i-2}) \\ + \rho_{i+1/2}(\phi_{i+1} - \phi_i) - \rho^* u^* \Delta x) \end{aligned} \quad (13)$$

At the second shock point, the corresponding equation is

$$\begin{aligned} c_{i+1/2}(\delta \phi_{i+1} - \delta \phi_i) - c_{i-1/2}(\delta \phi_i - \delta \phi_{i-1}) - c_{i-3/2}(\delta \phi_{i-1} - \delta \phi_{i-2}) \\ = -(\rho_{i+1/2}(\phi_{i+1} - \phi_i) - \rho_{i-1/2}(\phi_i - \phi_{i-1}) \\ - \rho_{i-3/2}(\phi_{i-1} - \phi_{i-2}) + \rho^* u^* \Delta x) \end{aligned} \quad (14)$$

It is clear from Eqs. (13) and (14) that the formation of a compression shock is allowed.

In general, a pentadiagonal solver is needed to simulate the flowfield. Only flows from left to right are considered here. In Fig. 1, a flow with an expansion shock as the initial condition is shown. The exact sonic solution is recovered (maximum residual $\sim 10^{-12}$) after 21 iterations. For flows with compression shocks, it is found that ϕ becomes discontinuous at the shock position after each iteration, as shown in Fig. 2.

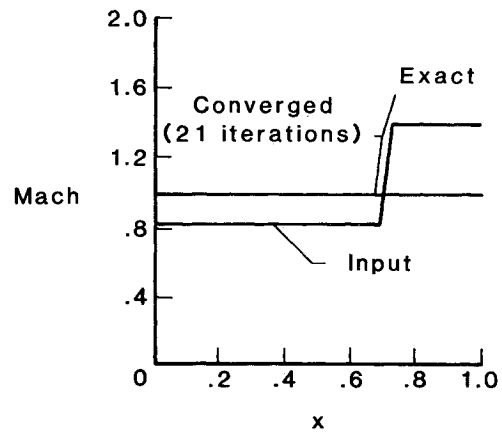


Fig. 1 Elimination of one-dimensional expansion shock.

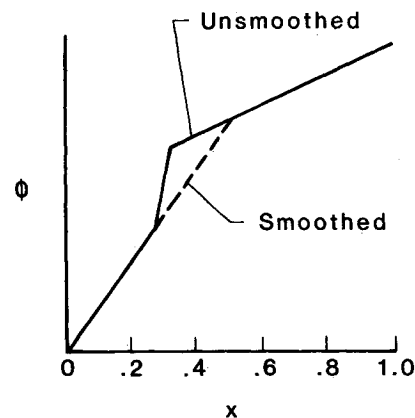


Fig. 2 Smoothing of a typical discontinuous potential solution.

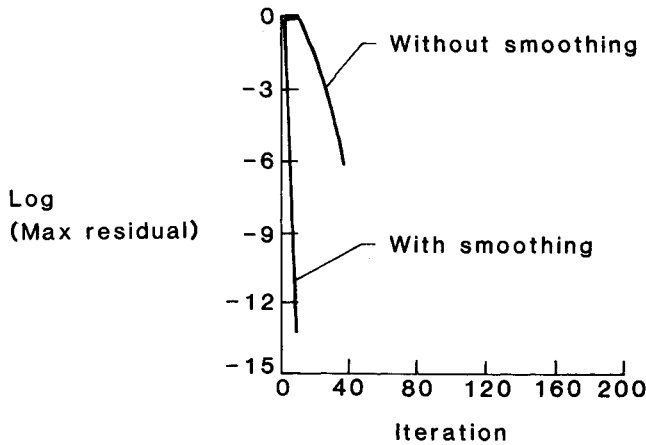


Fig. 3 Convergence of solution with and without smoothing.

Assuming that the shock is located at x_0 , the jump in ϕ at x is given by

$$\begin{aligned} [\phi]_{x_1} &= (\phi_u + \phi_{x_u}(x_1 - x_0) + \dots)_{x_0} - (\phi_d + \phi_{x_d}(x_1 - x_0) + \dots)_{x_0} \\ &= [\phi]_{x_0} + (x_1 - x_0)[\phi_x]_{x_0} + \dots \end{aligned} \quad (15)$$

where ϕ_u is the value of ϕ upstream of the shock at x_0 , and ϕ_d is the corresponding value downstream of x_0 . In order to make ϕ continuous, i.e., $[\phi]_{x_1} = 0$, x_1 should be such that

$$x_1 - x_0 = -[\phi]_{x_0} / [\phi_x]_{x_0} \quad (16)$$

Equation (16) provides a simple relation to move the shock and smooth the potential function. The smoothing technique was tested for the one-dimensional problem and the shock moved as many as 13 grid points per iteration, while the calculations remained stable. This allowed the shock to rapidly move to its final position and thus accelerated convergence, as demonstrated in Figs. 3–5. A similar procedure was reported recently in Ref. 17 where a Newton multigrid method was used to solve the full potential equation.

A final remark about the similarity of such a smoothing technique and shock fitting is in order. In Newton's method, the Jacobian is evaluated using information from the previous iteration and the correction is calculated to conserve mass assuming that the shock is frozen at the previous location. The other jump condition, $[\phi] = 0$, may not be satisfied. Thus, the present algorithm consists of locating the shock (where the viscosity is switched off), satisfying the jump conditions in two steps—conserving mass, and then moving the shock to obtain a continuous potential function using Eq. (16). Equation (16) is consistent, however, with the weak solution of

$$\phi_{xt} = \phi_{tx} \quad (17)$$

namely,

$$[\phi_x] \Delta x = -\Delta t [\phi_t] \quad (18)$$

The right-hand side of Eq. (18) is $\Delta t [\phi_t] = [\delta\phi]$ and assuming that the previous solution ϕ^n is continuous, it follows that $[\delta\phi] = [\phi]$, where $\phi = \phi^n + \delta\phi$.

Two-Dimensional Flows

For steady inviscid flows governed by the Euler equations, expansion shocks, as well as compression shocks, are possible. However, the entropy generated across expansion shocks is negative, while the change in entropy across compression

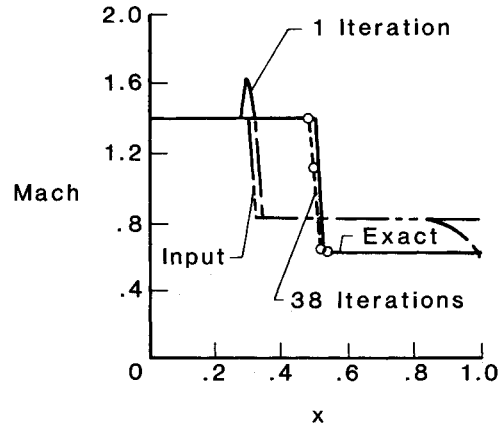


Fig. 4 Calculation of compression shock without smoothing.

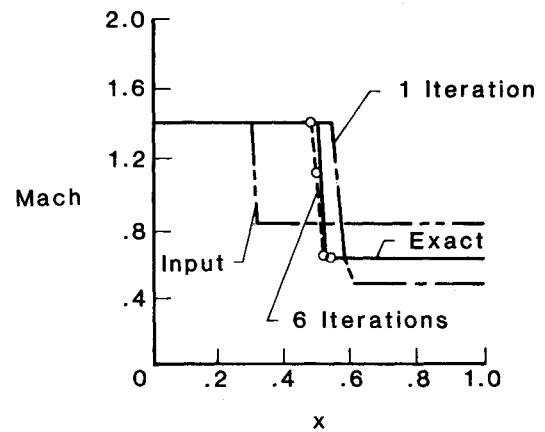


Fig. 5 Calculation of compression shock with smoothing.

shocks is positive. Hence, there is a direct way to exclude expansion shocks by imposing an entropy inequality.

For isentropic flows, it is not obvious how to construct such an inequality. It can be argued that since all the quantities are not conserved across the shock, the loss or the gain of a certain function may be analogous to the entropy production for Euler systems. Thus, a criterion for uniqueness of isentropic flows can be established.

This idea has been pursued in Ref. 6. The solution of the full potential equation is considered as the asymptotic limit of an unsteady hyperbolic system of conservation laws, endowed with a generalized convex entropy function, in the sense of Lax.⁷ Such a system can be written as

$$w_t + f_x + g_y = 0 \quad (19)$$

where any real linear combination of the Jacobian matrices has real eigenvalues and a complete set of eigenvectors. Moreover, when w is smooth, there exists a scalar convex function $V(w)$ that satisfies

$$V_t + F_x + G_y = 0 \quad (20)$$

where V is the entropy and F and G the associated entropy fluxes. Lax has shown that a necessary condition for a nonsmooth weak solution of Eq. (19) to be the limit (as $\epsilon \downarrow 0$) of solutions to the regularized equation

$$w_t + f_x + g_y = \epsilon (w_{xx} + w_{yy}) \quad (21)$$

is that the entropy inequality

$$V_t + F_x + G_y \leq 0 \quad (22)$$

must be satisfied.

In Ref. 8, it is shown that the Hessian of V symmetrizes the original system. The converse is also true¹⁸; a convex function serves as an entropy function if its Hessian symmetrizes the Jacobian matrices.

There are some difficulties in applying the above theorems to potential flows. Consider for example the unsteady potential equations

$$\rho_t + (\rho u)_x + (\rho v)_y = 0 \quad (23)$$

$$a^2/(\gamma-1) + \frac{1}{2}(u^2 + v^2) + \phi_t = k(t) \quad (24)$$

Equations (23) and (24) can be written in the form of a system of conservation laws

$$\begin{pmatrix} \rho \\ u \\ v \end{pmatrix}_t + \begin{pmatrix} \rho u \\ \frac{1}{2}(u^2 + v^2) + \frac{a^2}{\gamma-1} \\ 0 \end{pmatrix}_x + \begin{pmatrix} \rho v \\ 0 \\ \frac{1}{2}(u^2 + v^2) + \frac{a^2}{\gamma-1} \end{pmatrix}_y = \begin{pmatrix} 0 \\ 0 \\ 0 \end{pmatrix} \quad (25)$$

Except for one-dimensional flows, this is not a well-posed hyperbolic system. In Ref. 6, the following pseudo-unsteady system is used:

$$\begin{aligned} -\rho_t &= (\rho q \cos \theta)_x + (\rho q \sin \theta)_y \\ \theta_t &= -(q \sin \theta)_x + (q \cos \theta)_y \end{aligned} \quad (26)$$

where $u = q \cos \theta$ and $v = q \sin \theta$. Equation (26) can be written as

$$E w_t + A w_x + B w_y = 0 \quad (27)$$

where

$$\begin{aligned} E &= \begin{bmatrix} \rho q/a^2 & 0 \\ 0 & 1 \end{bmatrix} \\ -A &= \begin{bmatrix} \rho(1-M^2) \cos \theta & -\rho q \sin \theta \\ -\sin \theta & -q \cos \theta \end{bmatrix} \\ -B &= \begin{bmatrix} \rho(1-M^2) \sin \theta & \rho q \cos \theta \\ \cos \theta & -q \sin \theta \end{bmatrix} \end{aligned}$$

If Eq. (27) is multiplied by the matrix

$$\begin{bmatrix} 1/\rho q & 0 \\ 0 & 1 \end{bmatrix}$$

the resulting system is symmetric hyperbolic. This matrix is the Hessian of the convex function $V = P(q) + \frac{1}{2}\theta^2$, where $P''(q) = 1/\rho q$. The corresponding discrete entropy inequality is used in Ref. 6. It is not clear, however, how this result can be extended to three-dimensional or unsteady flows.

It is not even clear (for these cases) that the potential differential equation augmented with an artificial viscosity term in conservation form will admit only compression shocks as a weak solution. As mentioned before, the true unsteady potential formulation, for example, does not lead to a well-posed hyperbolic system and an entropy function in the sense of Lax may not exist.

In the potential formulation, mass and energy are conserved; momentum, however, is not conserved. Instead, entropy and vorticity are conserved (the flow is isentropic and irrotational). Consider the normal momentum jump across an Euler shock in one-dimensional flow

$$[\rho u^2 + p] = 0$$

Since

$$\rho = \rho_i e^{-\Delta s/R}$$

$$p = p_i e^{-\Delta s/R}$$

where ρ_i and p_i are the density and the pressure obtained from the isentropic formula.⁸ Since $[AB] = \langle A \rangle [B] + [A] \langle B \rangle$,

$$[\rho_i u^2 + p_i] \langle e^{-\Delta s/R} \rangle = -\langle \rho_i u^2 + p_i \rangle [e^{-\Delta s/R}]$$

This relation shows that $[\rho_i u^2 + p_i]$ has the same sign as $\Delta s/R$. It is also true that, for potential flows, the jump in momentum across the shock is positive for compression shocks and is negative for expansion shocks. (See, for example, Ref. 19.) To show this, let $q = \nabla \phi$ and n and t be normal to and tangential to the shock, respectively. Across the shock

$$[\rho q_n] = 0, \quad [q_t] = 0 \quad (28)$$

$$[h + \frac{1}{2}q^2] = 0 \quad (29)$$

where $h = \gamma p/(\gamma-1)\rho$. Let

$$\Delta = [\rho q_n^2 + p], \quad m = \rho q_n, \quad \tau = 1/\rho$$

and

$$[h] = \int dh = \int \frac{1}{\rho} dp = \bar{\tau} \int dp = \bar{\tau} [p]$$

Since the flow is isentropic, $1/\rho$ is a convex function of p , and $\bar{\tau} \leq \frac{1}{2}(\tau_1 + \tau_2)$. From Eqs. (28) and (29)

$$[h] = -\frac{1}{2}[q_n^2] = -\frac{1}{2}m^2[\tau^2] \quad (30)$$

Hence,

$$\bar{\tau}[p] = -m^2 \langle \tau \rangle [\tau] \quad (31)$$

and

$$\begin{aligned} \bar{\tau}\Delta &= -m^2 \langle \tau \rangle [\tau] + m^2 [\tau] \bar{\tau} \\ &= m^2 [\tau] (\bar{\tau} - \langle \tau \rangle) \end{aligned} \quad (32)$$

A global condition which excludes expansion shocks is then¹⁹

$$I = \int_{\Omega} \text{grad} \rho q \cdot D d\Omega \geq 0 \quad (33)$$

$$p_i = \frac{\rho_i^\gamma}{\gamma M_\infty^2} = \frac{\{1 - [(\gamma-1)/2] M_\infty^2 (u^2 + v^2 - 1)\}^{\gamma/(\gamma-1)}}{\gamma M_\infty^2}$$

where q is the velocity vector and D the momentum tensor $pI + \rho q \times q$. Applying the divergence theorem, I becomes

$$I = - \int \rho q \cdot \text{div} D d\Omega + \int_{\text{shocks}} [\rho q \cdot D \cdot n] ds \quad (34)$$

Since $\text{div} D = q \cdot \text{div} \rho q = 0$, the first term vanishes and

$$I = \int_{\text{shocks}} [\rho q_n (p + \rho q_n^2)] ds \quad (35)$$

On the other hand, with the proper artificial dissipation, a smooth potential solution (with large gradients in the shock region) should satisfy the following inequality:

$$\rho u [(\rho u^2 + p)_x + (\rho uv)_y] + \rho v [(\rho uv)_x + (\rho v^2 + p)_y] \geq 0 \quad (36)$$

Integrating over the field and using the relations

$$\rho u u_x + \rho v u_y = -p_x$$

$$\rho u v_x + \rho v v_y = -p_y$$

yields

$$\iint \rho (u^2 + v^2) [(\rho u)_x + (\rho v)_y] dx dy \geq 0 \quad (37)$$

It will be shown that with the present scheme, the inequality equation (37) is satisfied (under some restrictions).

A Modified Artificial Density Method

The artificial dissipation can be introduced by modifying the density based on flux biasing. In the present method, the regularized equation has the form

$$(\bar{\rho} \phi_x)_x + (\bar{\rho} \phi_y)_y = 0 \quad (38)$$

where

$$\bar{\rho} = (\rho q - \epsilon F_s)/q, \quad \epsilon = O(\Delta x)$$

$$F = \rho q \quad M > 1$$

$$= \rho^* q^* \quad M \leq 1$$

and

$$\frac{\partial F}{\partial s} = \frac{u}{q} \frac{\partial F}{\partial x} + \frac{v}{q} \frac{\partial F}{\partial y}$$

Multiplying Eq. (38) by ρq^2 and integrating by parts (assuming the flow is uniform or subsonic at the boundary of the domain of integration) yields

$$\begin{aligned} \iint \rho q^2 [(\rho u)_x + (\rho v)_y] dx dy &= - \iint (\rho q^2)_s F_s \epsilon dx dy \\ &= - \iint (2 - M^2) \rho q q_s^2 F_q \epsilon dx dy \end{aligned} \quad (39)$$

where $\rho_s = -(\rho/a^2) q q_s$.

Since $F_q \leq 0$, the right-hand side of Eq. (39) is non-negative [i.e., the inequality equation (37) is satisfied] if

$$M^2 < 2 \quad (40)$$

The constraint on the Mach number is not critical; the potential approximation is usually not acceptable if the Mach number upstream of a shock is greater than 1.3. Nevertheless, this restriction can be removed. If the full

potential equation is multiplied by q instead of ρq^2 , the result is

$$\begin{aligned} \iint q [(\rho u)_x + (\rho v)_y] dx dy &= - \iint q_s F_s \epsilon dx dy \\ &= - \iint q_s^2 F_q \epsilon dx dy \end{aligned} \quad (41)$$

The left-hand side of Eq. (41) is proportional to the drag or the difference in momentum ($\rho q^2 + p$), where it is assumed that the relation $\rho q q_s = -p_s$ is valid for smooth flows. The discrete analogue of Eq. (38) leads, however, to sharp shocks, as demonstrated by the numerical results, due to the implicit switch in the artificial dissipation.

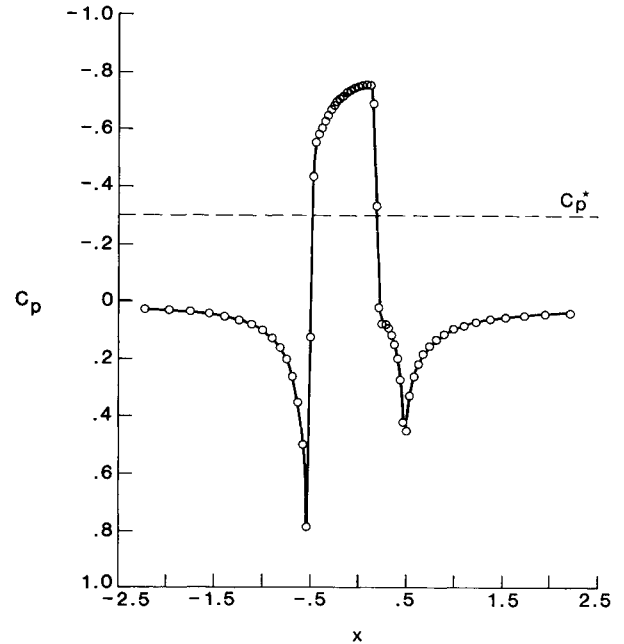


Fig. 6 Pressure distribution on NACA 0012 at $M_\infty = 0.85$ and $\alpha = 0$ deg (Cartesian grid).

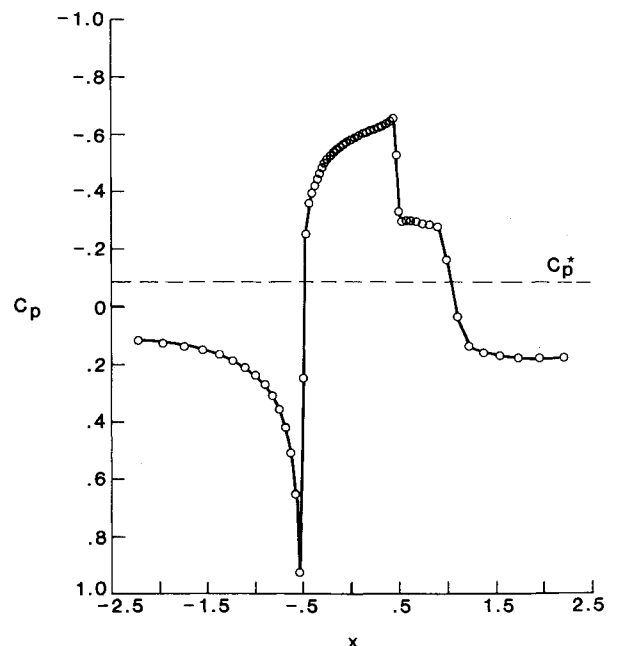


Fig. 7 Pressure distribution on NACA 0012 at $M_\infty = 0.95$ and $\alpha = 0$ deg (Cartesian grid).

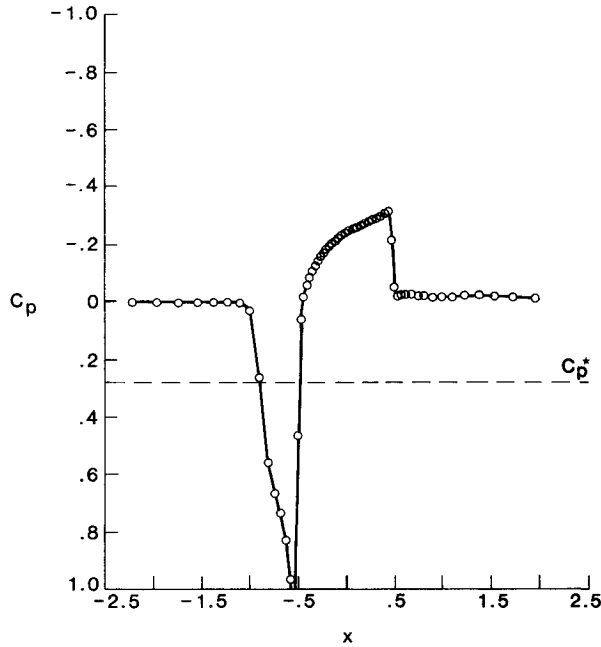


Fig. 8 Pressure distribution on NACA 0012 at $M_\infty = 1.2$ and $\alpha = 0$ deg (Cartesian grid).

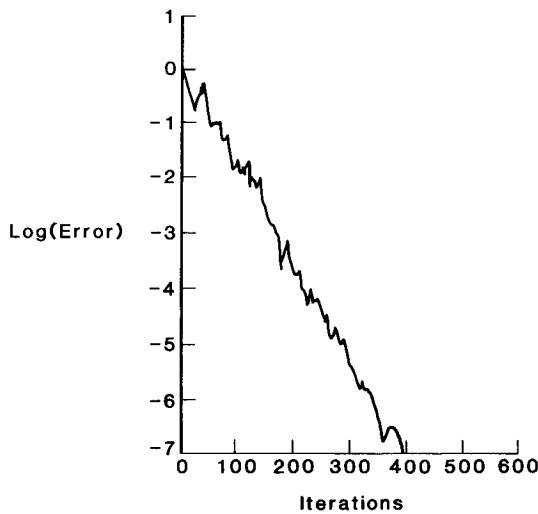


Fig. 9 Convergence rate and pressure distribution for NACA 0012 at $M_\infty = 0.80$ and $\alpha = 0$ deg (body-fitted coordinates).

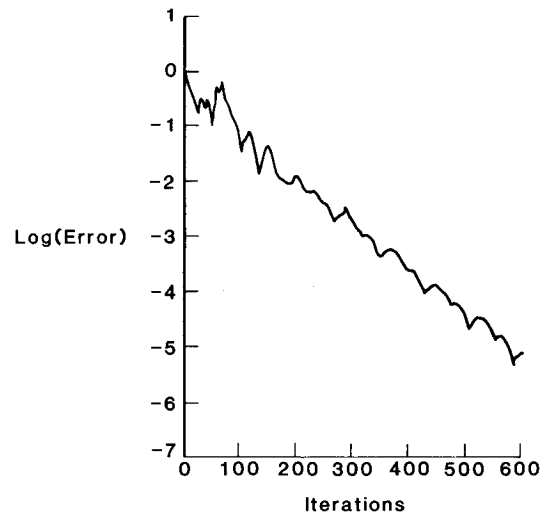


Fig. 10 Convergence rate and pressure distribution for NACA 0012 at $M_\infty = 0.75$ and $\alpha = 2$ deg (body-fitted coordinates).

A scheme with uniform viscosity, if it is *stable*, will lead to smeared shocks. For example, the conservative full potential analog of the Cole-Sichel viscous transonic equation²⁰ is

$$(\rho\phi_x)_x + (\rho\phi_y)_y = -\left(\frac{u}{q}\epsilon\phi_{ss}\right)_x - \left(\frac{v}{q}\epsilon\phi_{ss}\right)_y \quad (42)$$

where

$$\phi_{ss} = \frac{u^2}{q^2}\phi_{xx} + 2\frac{uv}{q^2}\phi_{xy} + \frac{v^2}{q^2}\phi_{yy}$$

To compare it with the present scheme, Eq. (42) can be written in the form

$$(\bar{\rho}\phi_x)_x + (\bar{\rho}\phi_y)_y = 0 \quad (43)$$

where

$$\bar{\rho} = (\rho q + \epsilon\phi_{ss})/q$$

Numerical results based on a similar scheme are reported in Ref. 21, where the discontinuity is smoothed and is spread over many points.

The drag associated with the uniform viscosity scheme is

$$\iint q [(\rho\phi_x)_x + (\rho\phi_y)_y] dx dy = + \iint \epsilon\phi_{ss}^2 dx dy \quad (44)$$

Needless to say, the conservative form of the governing equation is essential to recover the right jump conditions in the limit of vanishing grid size. The conservative form of the viscous term is necessary; otherwise, a net source is introduced and affects the results.

Finally, it should be mentioned that, in general, the discrete system may not have the same behavior as the differential equation. For example, in small-disturbance calculations, if the viscous term $(u^2)_{xx}$ is forward differenced instead of backward differenced, an expansion shock is produced.¹⁰ Although both differences are first-order approximations of the differential term, the truncation errors are completely different. In the absence of a discrete analysis, it is assumed here that, with proper differencing, the discrete system behaves in the same manner as the differential system—particularly if the flux function is differentially continuous.

Numerical Examples

First, the present scheme for the full potential equation is tested using Cartesian coordinates and linearized boundary conditions. The results for an x, y grid of 64×32 points are presented in Figs. 6–8. Next, TAIR,²² a computer code for solving the full potential equation using body-fitted coordinates, is modified according to Eq. (38). Results are shown in Figs. 9 and 10. The above calculations are based on the Zebra relaxation of Ref. 23.

Conclusions

The present scheme is simple to program, is parameter free, and leads to reliable calculations. A second-order accurate version (except in the shock region) can be achieved by using a weighted three-point formula for the F_s term in the definition of $\bar{\rho}$ in Eq. (38). Also, at the sonic line, a smooth transition is assured if proper averaging (or more viscosity) is used.

Applications of the present scheme to the unsteady full potential equation are reported in Ref. 24.

In a future paper, a completely second-order scheme, combined with a Newton linearization procedure (to guarantee quadratic convergence) will be reported.

References

- Engquist, B. and Osher, S., "Stable and Entropy Satisfying Approximations for Transonic Flow Calculations," *Mathematics of Computations*, Vol. 34, No. 149, 1980, pp. 45–75.
- Goorjian, P. and van Buskirk, R., "Implicit Calculations of Transonic Flow Using Monotone Methods," AIAA Paper 81-0331, 1981.
- Goorjian, P., Meagher, M., and van Buskirk, R., "Monotone Implicit Algorithms for the Small Disturbance and Full Potential Equation Applied to Transonic Flow," AIAA Paper 83-0371, 1983.
- Boerstoel, J., "A Multigrid Algorithm for Steady Transonic Potential Flows around Airfoils Using Newton's Iteration," *Journal of Computational Physics*, Vol. 48, 1982, pp. 313–343.
- Osher, S. and Engquist, B., "Upwind Difference Schemes for Systems of Conservation Laws—Potential Flow Equations," University of Wisconsin, Madison, MRC Rept. 2186, 1980.
- Osher, S., Hafez, M., and Whitlow, W. Jr., "Entropy Satisfying Approximations for the Full Potential Equation of Transonic Flow," *Mathematics of Computation*, Vol. 44, Jan. 1985, pp. 1–30.
- Lax, P., "Shock Waves and Entropy," *Proceedings of Symposium at the University of Wisconsin*, edited by E. Zarantonello, University of Wisconsin Press, Madison, 1971, pp. 603–634.
- Friedrichs, K. and Lax, P., "Systems of Conservation Laws with a Convex Extension," *Proceedings of the National Academy of Science USA*, Vol. 68, 1971, pp. 1686–1688.
- Murman, E. and Cole, J., "Inviscid Drag at Transonic Speeds," AIAA Paper 74-540, 1974.
- Steger, J. and Baldwin, B., "Shock Waves and Drag in the Numerical Calculation of Isentropic Transonic Flow," NASA TN D-6997, Oct. 1972.
- Garabedian, P., "Computation of Wave Drag for Transonic Flow," *Journal d'Analyse Mathématique*, Vol. 30, 1976, pp. 164–171.
- Garabedian, P. and McFadden, G., "Design of Supercritical Swept Wings," *AIAA Journal*, Vol. 20, March 1982, pp. 289–291.
- Murman, E., "Analysis of Embedded Shock Waves Calculated by Relaxation Methods," *AIAA Journal*, Vol. 12, May 1974, pp. 626–633.
- Jameson, A., "Transonic Potential Flow Calculations Using Conservation Form," *Proceedings of AIAA 2nd Computational Fluid Dynamics Conference*, AIAA, New York, 1975, pp. 148–155.
- Hafez, M. and Cheng, H. K., "Shock Fitting Applied to Relaxation Solutions of Transonic Small Disturbance Equations," *AIAA Journal*, Vol. 15, June 1977, pp. 786–793.
- Moretti, G., "Waves and Numerical Analysis," *Recent Advances in Numerical Methods in Fluids*, Vol. 4, edited by W. Habashi, Pineridge Press, 1984, pp. 645–668.
- Boerstoel, J. and Kassies, A., "Integrating Multigrid Relaxation into a Robust Fast-Solver for Transonic Potential Flows around Lifting Airfoils," AIAA Paper 83-1855, 1983.
- Tadmor, E., "Entropy Functions for Symmetric Systems of Conservation Laws," ICASE Rept. 172139, June 1983.
- Chattot, J., "Condition d'unicité pour les écoulements irrotationnels stationnaires de fluide parfait compressible," *Comptes Rendus de l'Académie des Sciences, Paris*, Vol. 268A, 1978.
- Sichel, M., "Structure of Weak Non-Hugoniot Shocks," *The Physics of Fluids*, Vol. 6, 1968, pp. 653–663.
- Hafez, M. and Lovell, D., "Entropy and Vorticity Corrections for Transonic Flows," AIAA Paper 83-1926, 1983.
- Holst, T., "Implicit Algorithm for the Conservative Transonic Full-Potential Equation Using an Arbitrary Mesh," *AIAA Journal*, Vol. 17, Oct. 1979, pp. 1038–1045.
- Hafez, M. and Lovell, D., "Improved Relaxation Schemes for Transonic Potential Calculations," AIAA Paper 83-0372, 1983.
- Whitlow, W., Hafez, M., and Osher, S., "An Entropy Correction Method for Unsteady Full Potential Flows with Strong Shocks," NASA TM 87767, June 1986.